Detailed Characterization of Flow Disturbances Caused by SDBD Plasma Actuator

Alexander Frolov[1], Sergey B Leonov[1], Ivan Moralev[1], Victor Soloviev[1], Dmitry Opaits[2], Richard Miles[2]

[1] Joint Institute for High Temperature RAS, Moscow, 125412, Russia, leonov@ihed.ras.ru
[2] Princeton University, Princeton, 08540, NJ, USA

Introduction

The objective of this work is to analyze the details of SDBD spatial and temporal evolution in order to make clearer the physical mechanism of plasma-flow interaction and, finally, to maximize the local and instant amplitude of the plasma effect.

Over the past 10-15 years, many studies have been conducted on boundary layer (BL) actuation by surface dielectric barrier discharge (SDBD) [1-4]. These discharges directly act on gas momentum by the mechanism of charge separation and momentum transfer in collisions of electrons and ions with neutral gas molecules [5-8]. In most cases the average magnitude of the plasma-induced velocity is rather small and ineffective for high-speed flow control. Another mechanism for BL separation control by SDBD is the improvement of flow stability by the addition of disturbances to the BL at a particular frequency. In this regard the magnitude and time characteristic of the local plasma-induced thermal or non-thermal fluctuations may be more important than the amplitude or direction of discharge-induced gas movement [6-8].

The complex structure of the DBD discharges should obviously lead to onset of the 3D disturbances in the BL. Varying the parameters of the discharge (voltage and freq), one can vary the distance between streamers, therefore changing heat/force sources distribution, adapting it to the spatial wavelength required. Spatial structure of the surface DBD discharges, especially at high carrying frequencies, appears to be non-homogeneous. Due to the discharge volume instabilities, discharge constricts to a number of filaments with higher current densities. Micro-discharges spacing and behavior are ruled by two main processes: charge deposition on the dielectric surface and heating of the gas in the discharge channels. The last approach: generation of X-wise plasma streaks and their interaction with boundary layer, - may lead to production of intensive longitudinal vorticity in near-wall flow slice.

Body force generation

According to available experimental data the SDBD for alternating (usually sinusoidal) applied voltage waveform consists of a set of tens microdischarges repeating each a half cycle. For a stage of microdischarge generation at negative electrode polarity negative ions are mainly O^- ions [6], but for relaxation phase between microdischarges the type of negative ion changes onto O_2^-, O_3^- ions because of both a rapid conversion of O^- ions into O_2^-, O_3^- ions and additional production of O_2^-, ions in three-body electron attachment process. The body force equals to the product of volumetric charge and electric field. Because of three orders of magnitude difference between microdischarge building up time (few tens nanoseconds) and relaxation time between microdischarges (few tens microseconds), the main contribution into body force occurs at relaxation phase.

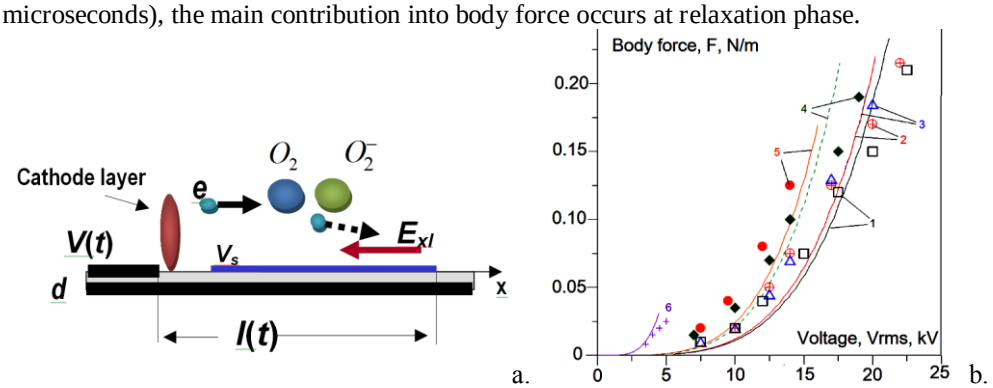

Fig. 1 (a) - the scheme of negative ion production and drifting along the surface charge layer; V(t) and Vs are potentials of exposed electrode and surface charge layer, small circle "e" denotes the electron; (b) - Theoretical estimation of the thrust per unit electrode lenght (lines) against experimental data [1] (symbols) for 1 – Teflon (ε =2), d = 6.35mm, f_v=2.1kHz; 2 – Derlin (ε =3.5), d = 6.35mm, f_v=2.3kHz; 3 – Quartz (ε =4.2), d = 6.35mm, f_v=2.3kHz; 4 – Teflon(ε =2), d = 3.18 mm, f_v=2 kHz; 5 – Macor (ε =6), d = 3.18 mm, f_v=2.3 kHz; 6 – Kapton (ε =3.9), d = 0.15 mm, f_v=4.4kHz; $V_{rms}=V_0/1.7$ (b)

The scheme of volumetric negative charge accumulation for discharge evolution at negative voltage is shown in Fig. 1a. For negative electrode polarity the main amount of electron-ion pairs is produced by ionization in a cathode layer. Electrons leave the cathode layer and drift along the dielectric surface because the normal component of electric field is zero due to its screening by the surface charge layer. On their drift way to the end of the surface charge layer in longitudinal electric field E_{xl} electrons could be attached to O_2 molecules and create O_2^- ions or reach the dielectric surface and increase the surface charge layer length. The created O_2^- ions drift along the dielectric surface much slower, because the mobility of negative ion is approximately two orders of magnitude less than electron mobility.

Estimations show [8] that for typical SDBD conditions the volumetric charge relaxation time due to ion drifting to dielectric surface is much greater than the time interval between microdischarges. This means that the charge of negative ions is accumulated during the microdischarge series. This assertion has been proved by numerical simulation [5] for a set of microdischarges driven by negative ramp voltage. Analytical analysis of the integral force per unit length of exposed electrode has been done in Ref. [8] on the basis of hypothesis, that the body force induced by SDBD plasma is mainly due to negative ion accumulation inside a volume above the dielectric. Predicted force dependences on applied voltage, dielectric thickness and its relative permittivity qualitatively coincide with experimental observation validating the applied hypothesis. The results of analytical prediction comparison against the experimental data [1] are shown in Fig. 1b.

Experiment 1: Z-inhomogeneity

The experimental approach includes time resolved pressure measurements of plasma-induced flow in air and in nitrogen, fast cam imaging, and PMA-based measurements of the parameters of the DBD luminosity. The tests were made in a conventional non-symmetrical electrode configuration of SDBD at voltage amplitude $V_0 \leq 12$kV and a sinusoidal/rectangular waveform with a variable frequency f = 0.02-5kHz [7]. The dielectric plate was made of MACOR™ with a thickness d = 1mm. In some tests a small (0.5-3mm in X direction) triangle tip was attached to the exposed electrode. To explore the behavior of the discharge luminosity area optical measurements of its length have been carried out simultaneously with the recording of the electrical parameters.

Spatial distribution of the discharge-related momentum. Large variations in the pressure signal along Z direction were observed. The plasma-induced flow field appears to be made up of a few individual jets, where the pressure signal amplitude is higher by a factor of 10 or more compared to other locations along the electrode. The typical gas velocity in these jets is U_{ind} = 1-5m/s, which corresponds to a measured pressure of about P=0.7-17Pa. No correlation of the DBD-jet position with streamers was found. The maximum effect was achieved with a small triangle tip attached to the exposed electrode. The spatial distribution of the maximum signal at positive and negative polarities of the voltage applied is rather complex as shown in Fig.2 for a plain electrode (a) and for a tipped electrode (b). Only powerful streamers' corona (which is certainly observed by high-speed camera) originating in higher electric fields near an electrode tip could produce a body force comparable with a force, generated at negative polarity of electrode.

Nitrogen vs Air. These comparisons are the most impressive: there was no pressure signal under negative slope of the voltage at all on either the tipped or the plain exposed electrode in pure nitrogen.

Maximum pressure signal. Under the conditions of this experiment the maximum amplitude of the pressure signal was measured in air for the electrode with a tip. The value of this pressure corresponds to induced flow velocity V_{max}=12.5m/s. No notable variation of the time-averaged local plasma-induced pressure has been detected on the tipped electrode with supplying voltage frequency variation in the range of 20-2000Hz.

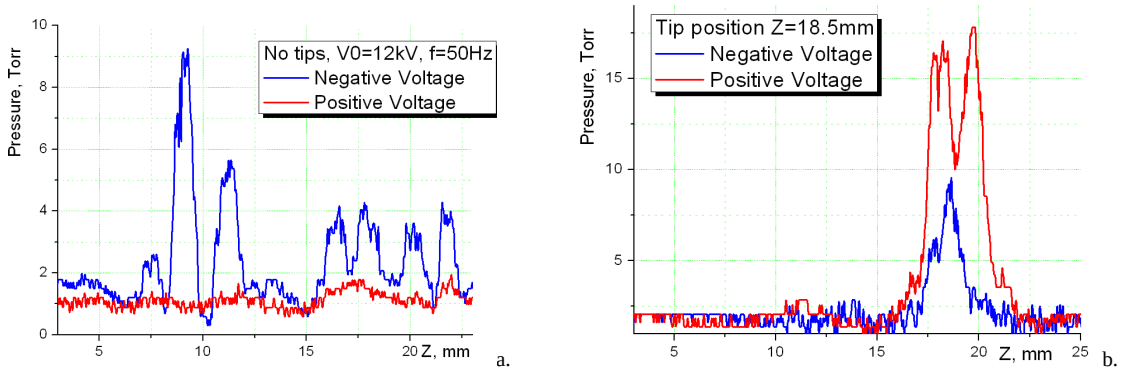

Fig. 2 Amplitude of the pressure along the exposed electrode. Plain (a) vs tipped electrode (b).

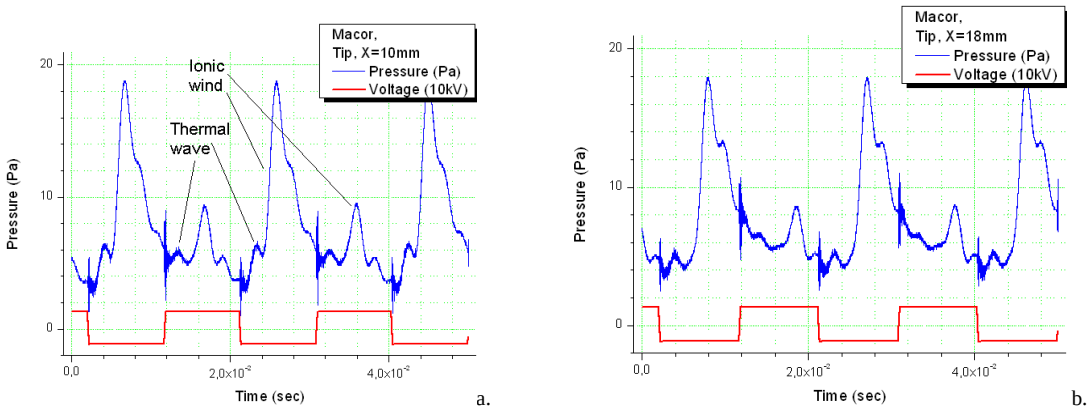

Fig. 3 Pressure signal in Air at electrode with the tip, X = 10 (a) and 18 (b) mm.

Rectangle vs Sinusoidal. The application of a rectangular voltage waveform to the DBD results in a pressure signal with a sharper leading edge. It allows the identification of two types of features in the pressure trace: those induced by the thermal driving force and those induced by ionic wind. As indicated in Fig.3, a thermal push impacts the sensor the first. The second wave, arriving after the thermal wave, is the ionic wind and has a velocity of several m/s. It seems that the "negative" DBD-jet is narrower, than the "positive" one, because it keeps the momentum for a longer distance.

Experiment 2: Plasma Streaks

It is well known fact that increase of power release in SDBD leads to discharge contraction. However, study of the constricted regime is usually omitted. In this work the SDBD was studied in air on a 5 mm thick ceramics (ε=3.9) substrate, at the following conditions: power release W=0.1 - 0.8 kW; feeding frequency 70 - 450kHz; air pressure 1Bar.

The discharge spatial structure, captured by high-speed camera, at carrying frequency 450kHz is shown in Fig.4. Three main modes were obtained: quasihomogeneous, constricted with evenly spaced channels and constricted with chaotically distributed channels. Transition from the first mode to the second one occurs as the formation of extra single current filaments; number of them increasing with the increase of the voltage magnitude. Finally, channels form an evenly spaced array on the electrode edge, with nearly equal gaps distribution. At further voltage raise the length of individual channels increases more and the branching of their fins is appeared visible. It should be noted that frequency elevation leads to reduction of the power required for the transition to the next discharge mode.

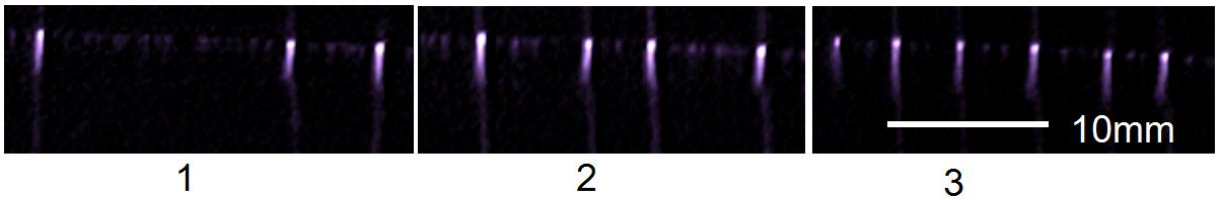

Fig. 4 Three different regimes of the discharge at increasing power (W3>W2>W1).

Concluding remarks

The experimental and analytical results reported here revealed some unique features of the surface dielectric barrier discharge evolution and its effect on the flow. The following outlines look currently to be important. First, a strong inhomogeneity of discharge-induced flow velocity Z-distribution along the electrode length has been found. This inhomogeneity is accompanied by a jump in the body force value for a voltage half-cycle with negative going potential, whereas the body force for a voltage half-cycle with positive going potential it remains approximately the same along the electrode. Second, the results confirm the important role of negative ions in actuator efficiency. In nitrogen the discharge induced pressure increase is zero for a voltage half-cycle with negative polarity, whereas in air it forms the main input to the body force. Third, the two types of gas disturbances due to DBD impact have been experimentally separated – the thermal effect and momentum transfer (ion wind) effect. The latter is much greater than the former. Finally, the discharge mode with equidistant distribution of the plasma streaks was demonstrated for the plane electrodes configuration for the first time. It could be very practical approach thinking about a longitudinal vorticity generation nearby the

contoured surfaces. These data could be useful at actuator design for BL separation/transition control and aerodynamic noise mitigation.

The experiments (section 1.3) were supported in part by Department of Mechanical Engineering of Princeton University. This work was also supported by Russian Foundation of Basic Research in the frame of projects 10-08-01056a and 12-08-00995a.

References

1. F. O. Thomas, T. C. Corke, et all (2009), AIAA Journal 47, 2169
2. E. Moreau, (2007) J. Phys. D: Appl. Phys. 40, 605 // N. Bénard, E. Moreau, AIAA 2012-3136
3. C. L.Enloe, M. G. McHarg, Th. E. McLaughlin, (2008) J.Appl.Phys. 103, 073302
4. U. Kogelschatz, (2010) Journal of Physics: Conference Series, vol. 257, 2010 IOP, p. 012015.
5. J. P. Boeuf, Y. Lagmich, Th. Unfer, et all, (2007) J. Phys. D: Appl. Phys. 40, 652
6. V. Soloviev, V. Krivtsov, (2009) J. Phys. D: Appl. Phys 42 125208
7. S. Leonov, R. Miles, D. Opaits, V. Soloviev (2010) PHYSICS OF PLASMAS 18, 6 (Oct)
8. V. Soloviev (2012) J. Phys. D: Appl. Phys. 45 025205